



Research on the joining of dissimilar aluminum alloys by a dieless clinching process

Denglin Qin^{1,2} · Chao Chen^{1,2}

Received: 28 February 2022 / Accepted: 11 August 2022 / Published online: 5 September 2022
© The Author(s), under exclusive licence to Springer-Verlag London Ltd., part of Springer Nature 2022

Abstract

The dieless clinching process is a newly proposed modified variation of the conventional clinching process, and it exhibits numerous merits when joining aluminum alloys. In this article, the dieless clinching process for joining dissimilar aluminum alloys was investigated experimentally. Three types of aluminum alloys, i.e., AL5052, AL5182, and AL6061, were used to produce the dieless clinched joints according to 6 types of sheet material arrangements. Geometrical and mechanical characterization of various joints were analyzed to assess the clinch-ability and mechanical property of these joints. The key geometric parameters, static tensile/shear strength, energy absorptions, and failure modes of these joints were obtained and discussed. The results show that the sheet with higher deformation resistance should be used as the upper sheet in the dieless clinched joint for better mechanical performance.

Keywords Joining · Aluminum alloys · Clinch-ability · Mechanical properties · Failure modes

1 Introduction

During the last few decades, the automobile industry has experienced a period of vigorous development, which also brought some problems such as environmental pollution and energy exhaustion. For this issue, governments around the world have been enacting strict laws regarding fuel consumption and tailpipe emission of cars to force traditional automobile manufacturers to transform and upgrade [1]. It is reported that a 10% vehicle weight reduction brings about a 6~8% fuel consumption reduction. Therefore, it is an urgent task for automakers to develop light-weighting technologies in automotive manufacturing. Generally, there are three approaches to achieving lightweight of vehicles, i.e., using lightweight materials, optimizing structure design, and developing advanced manufacturing technology [2]. Among these approaches, the use of advanced lightweight

materials including aluminum alloys, magnesium alloys, titanium alloys, etc. is recognized as the most effective one for reduction of fuel consumption and emissions. Due to their superior properties of high specific strength, strong corrosion resistance, good processability, and relatively low cost, aluminum alloys have acquired progressively extensive interest from automotive industries [3]. On the other hand, although some automobile manufacturers, i.e., Tesla, have attempted to adopt the integral structural parts in automobile manufacturing to achieve extreme weight reduction, it is still the first choice for most car manufacturers to adopt connected structures for lower processing difficulty and cost [4]. At present, resistance spot welding (RSW) is the dominant joining process in automobile manufacturing and there exist roughly 4000–5000 RSW joints in a typical body in white [5]. However, it is quite tough to join aluminum alloys by RSW due to their characteristics of low melting point and high thermal conductivity. Therefore, some advanced connecting technologies suitable for joining aluminum alloys should be proposed and developed.

Mechanical clinching, presented in 1897 firstly and applied in practice after the 1980s, can directly join sheets by inducing sheets to deform locally and form a geometrical interlock structure [6]. Over the last decade, the clinching process has developed rapidly and has been increasingly widely used in the fields of automobile and household

✉ Chao Chen
profchenchao@163.com

¹ Light Alloy Research Institute, School of Mechanical and Electrical Engineering, Central South University, Changsha 410083, China

² State Key Laboratory of High Performance Complex Manufacturing, Central South University, Changsha 410083, China

appliances [7]. Compared with other joining techniques, e.g., welding, adhesive bonding, and traditional riveting, the clinching process has some superiorities such as no heat, splashes, or emissions produced, no auxiliary parts and pretreatment process required, and low operating cost [8].

In the last decade, in-depth research regarding mechanical clinching techniques was conducted and some modified clinching processes have been proposed and studied. Neugebauer et al. [9–11] utilized a planar anvil to replace the grooved die of the conventional clinching process. By this method, the heat transfer from the lower die to the sheets to be joined is facilitated, which contributes to the joining of metals with poor ductility (e.g., magnesium alloy). Ran et al. [12] investigated the rectangular shear clinching process, in which, a rectangle punch was adopted to cut sheets firstly and generate mechanical interlock between sheets secondly. The effect of various forming forces on the final rectangular shear clinched joints was revealed in their study. Compared with the conventional round clinched joint, the square clinched joint has higher plane torsion resistance. Hence, the square clinching process that uses a square punch and bottom die was also investigated by some scholars. Wang et al. [13] experimentally compared the optimum forming force range and static strength of conventional round clinched joints and square clinched joints. Gao et al. [14] carried out the square clinching process to join Al5052 sheets with various thicknesses. The mechanical strength, absorbed energy, and failure behaviors of various square clinched joints were compared and analyzed. The result

shows that the thicker sheet is more suitable as the upper sheet in the square clinching process for a better clinched joint. Roller clinching is a type of modified clinching process that can produce interlocks between sheets by rotational tool movement. Pan et al. [15] investigated the deformation features of roller-clinched joints using experimental and simulative methods. The processing parameters were also optimized by multiple linear regression analysis. He et al. [16] proposed a type of modified clinching process, i.e., rotated clinching process, in which two arc heads that can rotate in opposite directions were utilized to replace the punch in the conventional clinching process. The feasibility of this rotated clinching process for joining AL1060 sheets was testified, and the static strengths of joints under various descent distances of rotated heads were obtained.

Recently, the authors proposed a variant of conventional clinching, i.e., the novel dieless clinching process, by using a flat anvil and a shouldered punch instead of the fixed or split die with a groove and the blank holder-punch set in the conventional clinching process [17]. The die structure of the dieless clinching process is simple, which is in favor of equipment manufacturing and maintenance. Moreover, the flat anvil used makes it easy to guarantee the centring of the punch and lower die, which not only guarantees the joint quality but also alleviates the wear of the punch. The schematic of the dieless clinching process that involves 4 stages roughly is depicted in Fig. 1. A more detailed description regarding the dieless clinching process is presented in reference [17].

Fig. 1 Process sequence of the dieless clinching process: **a** localized deformation, **b** drawing, **c** interlocking forming, and **d** interlocking enlarging

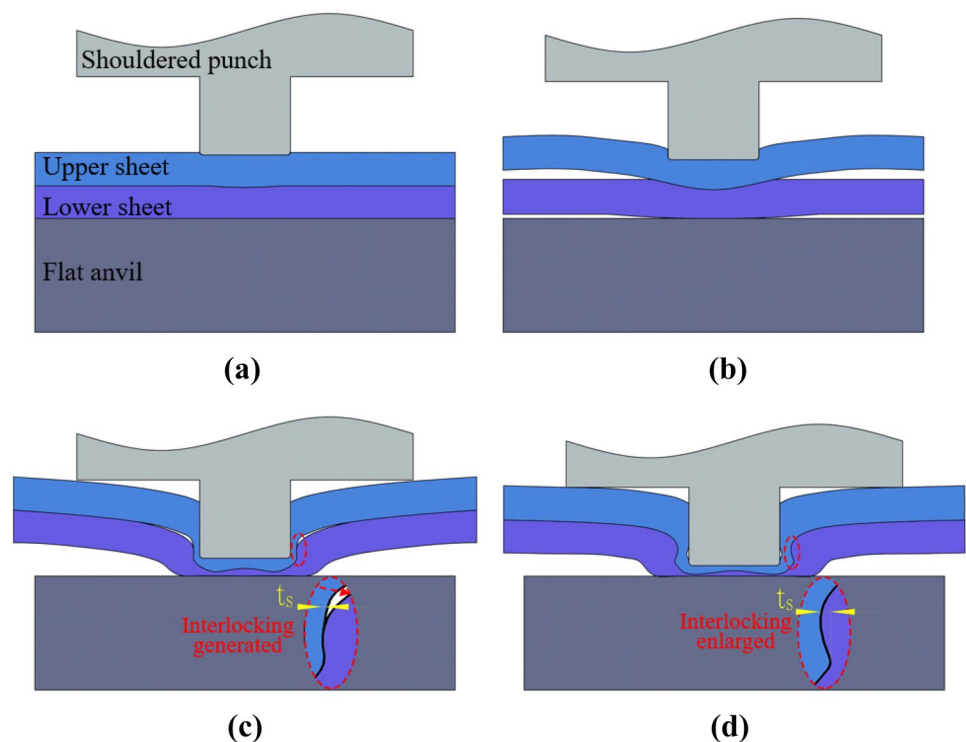


Table 1 Main mechanical properties of various aluminum alloy sheets

Material	Elastic modulus (GPa)	Yield strength (MPa)	Tensile strength (MPa)	Elongation	Poisson's ratio
AL5052-H32	62.1	158.7	228.6	16.5%	0.33
AL5182-O	66.2	151.1	311.9	20%	
AL6061-T6	67.1	302.2	327	9.2%	

The use of structures made of dissimilar materials for balancing functionality and cost is common in automobile manufacturing [18]. Therefore, more and more researchers applied the clinching process to joining dissimilar materials over the past few years. Lambiase et al. [19–22] have made a lot of fruitful attempts to join metals and polymers using the clinching process. From their study, it is relatively hard to produce metal-polymer joints using the clinching process at room temperature due to the low ductility and fragility of polymers, but pre-heating the sheets before clinching contributes to the formation of sound clinched joints. Ali and Benabderrahmane [23] studied the clinching process for connecting aluminum 5754 and other materials including copper, CuZn37, PS, extra mild steel, and high-strength steel using the finite element method. The result shows that the sheet material properties affect the forming force and mechanical properties of clinched joints significantly. Chu et al. [24] investigated the clinching process of aluminum, titanium, and galvanized steel sheets. It is reported that the sheet material arrangements have remarkable impacts on the joint strength and the sheet

material of high hardness and strength is more suitable as the upper sheet in the clinching process. Jung et al. [25] investigated the clinching process for joining Al6451 and Al7075. They found that when the aluminum alloy sheet with relatively low elongation (i.e., Al7075) was placed on the punch side, the clinched joint can not be produced due to the breakage of the upper sheet.

In the current research, the dieless clinching process for joining dissimilar aluminum alloys was investigated experimentally. Three types of aluminum alloys, i.e., AL5052, AL5182, and AL6061, which are commonly used in the automobile industry, were adopted to produce the dieless clinched joints. Six different joints, i.e., AL5052-AL5182, AL5182-AL5052, AL5052-AL6061, AL6061-AL5052, AL5182-AL6061, and AL6061-AL5182 joints were produced. Geometrical and mechanical characterization of various joints were analyzed to assess the clinch-ability and mechanical property of these joints. The results show that the dieless clinched joints with a hard upper sheet exhibit better performance in both clinch-ability and static mechanical properties.

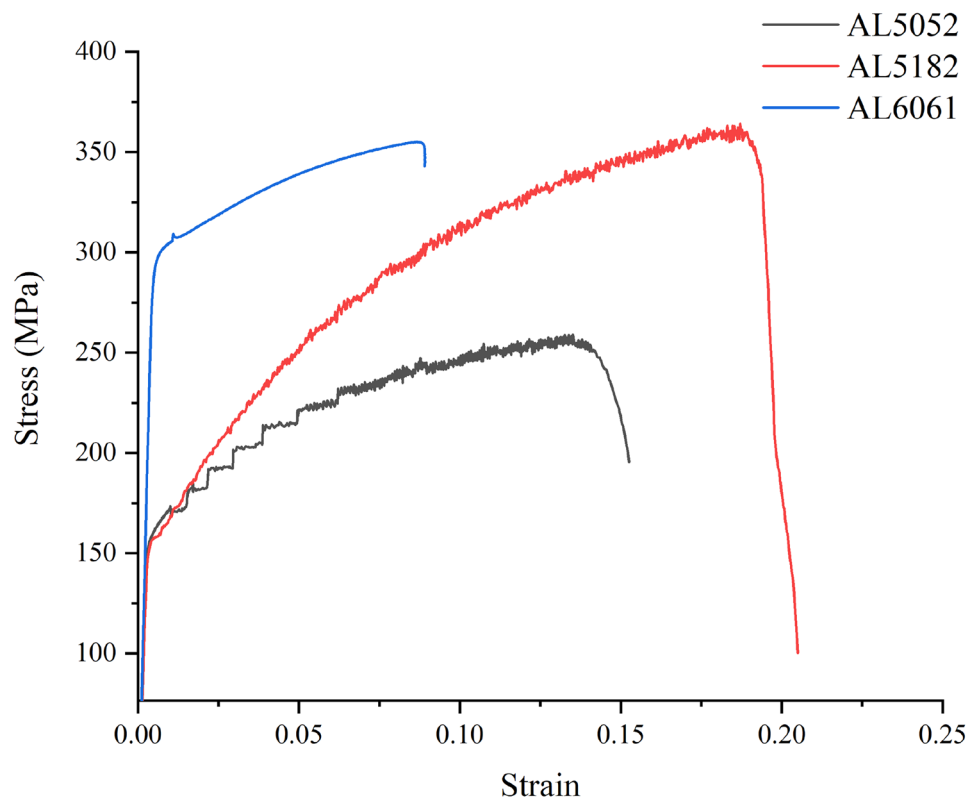
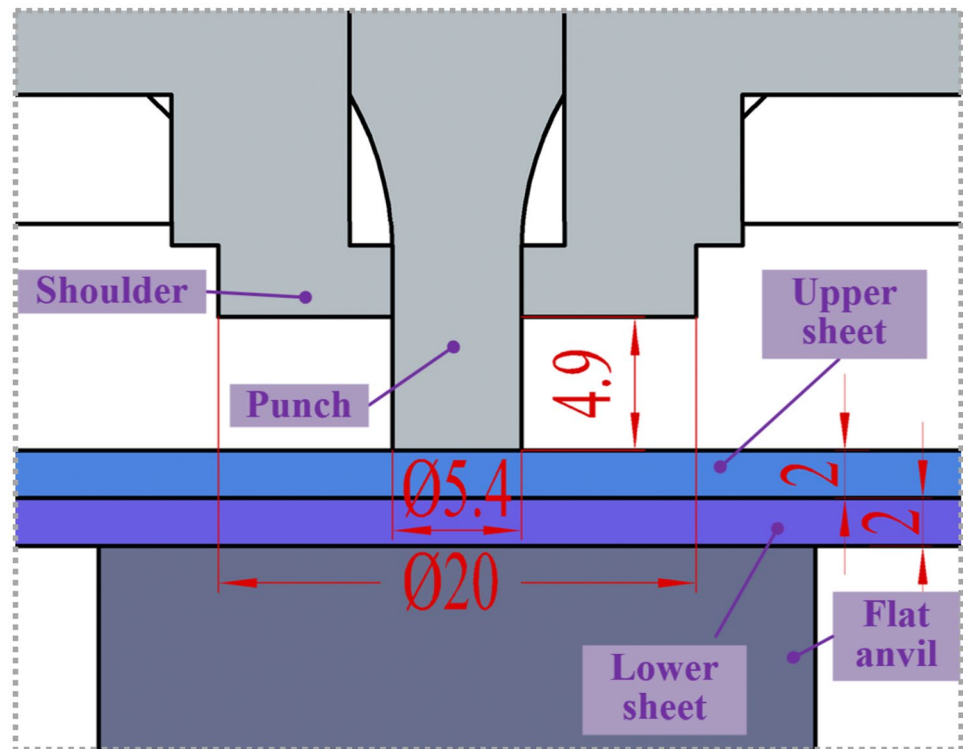
Fig. 2 True stress–strain curves of various aluminum alloy sheets

Fig. 3 Device of the dieless clinching process



2 Materials and methods

2.1 Materials

Three types of aluminum alloys, i.e., AL5052-H32, AL5182-O, and AL6061-T6 with 2 mm of thickness, were selected as the sheet materials in this study. For ensuring the uniform performance of each sheet material, all specimens of 80 × 25 mm (length × width) were cut from a large sheet. The mechanical characterization of these aluminum alloys was implemented by uniaxial tensile tests (according to GB/T 228.1–2010). A consistent tensile speed of 2 mm/min was set for all the tests. The main mechanical properties and true stress–strain curves of various aluminum alloy sheets were reported in Table 1 and Fig. 2, respectively. As can be noted from Table 1 and Fig. 2, for the same degree of plastic deformation, the order of resistance to deformation of these aluminum alloy sheets is AL5052 < AL5182 < AL6061.

2.2 The dieless clinching process

The dieless clinched joints were produced utilizing the device designed by the authors. Figure 3 shows the device of the dieless clinching process, which comprises three parts: the flat anvil, the shoulder, and the punch. The shoulder and the punch were assembled together and could reciprocate

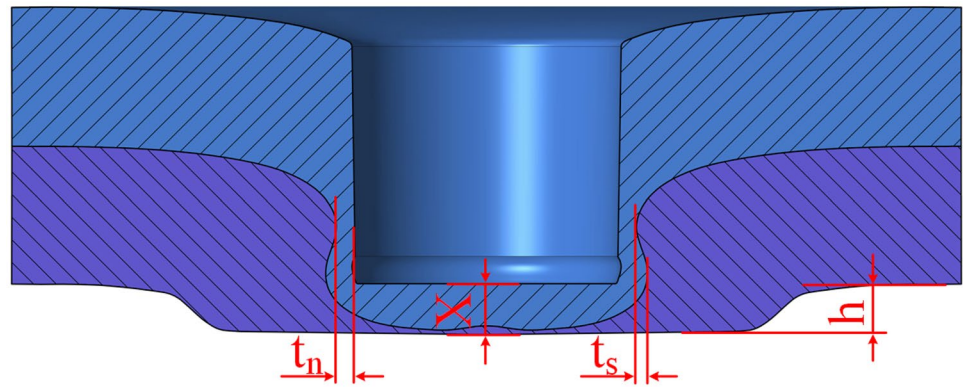
integrally (both the shoulder and punch correspond to the shouldered punch in Fig. 1). The key dimensions of the device were also reported in Fig. 3 (unit: mm). This device mentioned was mounted on the Sust CMT-5105GJ testing machine and during the clinching process, and the testing machine drove the punch to move downward to make the sheets generate the mechanical interlock.

For the clinching process of dissimilar aluminum alloys, the sheet arrangement sequence plays an essential role in the final joints produced. To this end, 6 types of arrangement of AL5052, AL5182, and AL6061 sheets were used to prepare the clinched joint as shown in Table 2. For each type of sheet arrangement, three levels of forming force, i.e., 60 kN, 68 kN, and 76 kN, were used. The forming speed kept consistent at 2 mm/min for all tests.

Table 2 Arrangement types of AL5052, AL5182, and AL6061 sheets

Nomenclature	Upper sheet	Lower sheet
A1	AL5052	AL5182
A2	AL5182	AL5052
B1	AL5052	AL6061
B2	AL6061	AL5052
C1	AL5182	AL6061
C2	AL6061	AL5182

Fig. 4 Cross-section of the dieless clinched joint



2.3 Geometrical and mechanical characterization of the dieless clinched joints

The geometrical characteristics of the clinched joints not only reflect the clinch-ability of sheet materials but also have a decisive effect on the mechanical properties and failure modes of final joints [26]. Hence, in this study, the geometrical characterization analysis of the dieless clinched joints was carried out. A diamond wire cutting machine was adopted to section the clinched joints along their centerlines to obtain the joint cross-sections. Then, an optical microscope with a measuring system was adopted to observe and measure the geometric characteristics of the joint cross-sections. The cross-section of the dieless clinched joint that mainly includes 4 key geometric parameters is depicted in Fig. 4. Among these four parameters, the neck thickness (denoted by “ t_n ”) and interlock value (denoted by “ t_s ”) directly determine the joint mechanical properties. The bottom thickness (denoted by “ X ”), which can be obtained by conventional thickness gauges, is commonly used for a quick inspection of joint quality. The protrusion height (denoted by “ h ”) that may affect the esthetics and functionality of structure or product with clinched joint, should be reduced in practical application.

In engineering applications, the joint load-bearing capacity is one of the most concerned properties. Therefore, two types of static mechanical tests, i.e., cross-tensile test and lap-shear test, were implemented to characterize the static mechanical performance of the dieless clinched joints in the case of 76 kN forming force. Figure 5 illustrates the specimen configurations in the two static mechanical tests. During the lap-shear test, two spacers with 2 mm thickness were stuck on both ends of the specimen to eliminate the undesired bending effect. The static mechanical tests upon clinched joints were also performed by the aforementioned Sust CMT-5105GJ universal tester. The testing machine was activated to apply load on the clinched joint until the joint was fully destroyed after the specimen was fixed on the clamps of the testing machine. For all tests, the speed of the testing machine was set to a consistent 2 mm/min. Three repeated tests for the joint of each sheet arrangement were conducted.

During the mechanical test process, the joint load force–displacement curve can be plotted by the testing machine system automatically. And some essential mechanical characteristics of clinched joints, e.g., stiffness K , strength F_{max} , and energy absorption En , can be reflected in the load force–displacement curve as depicted in Fig. 6.

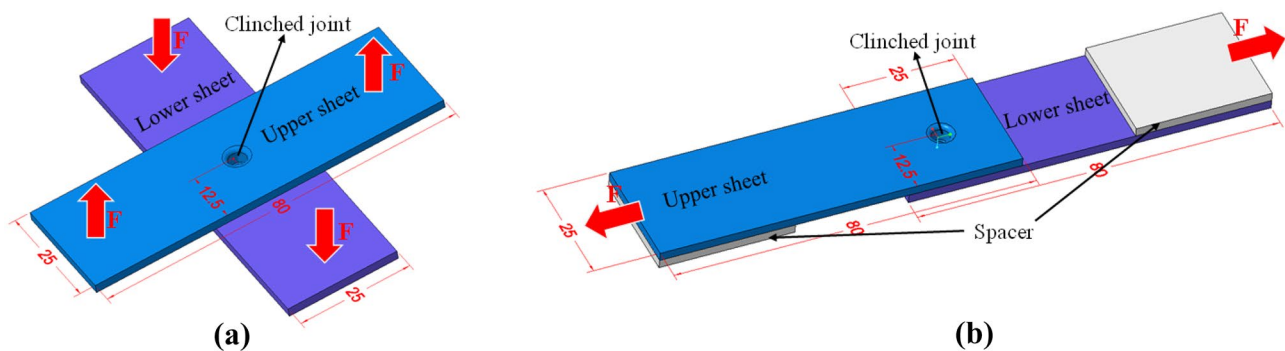
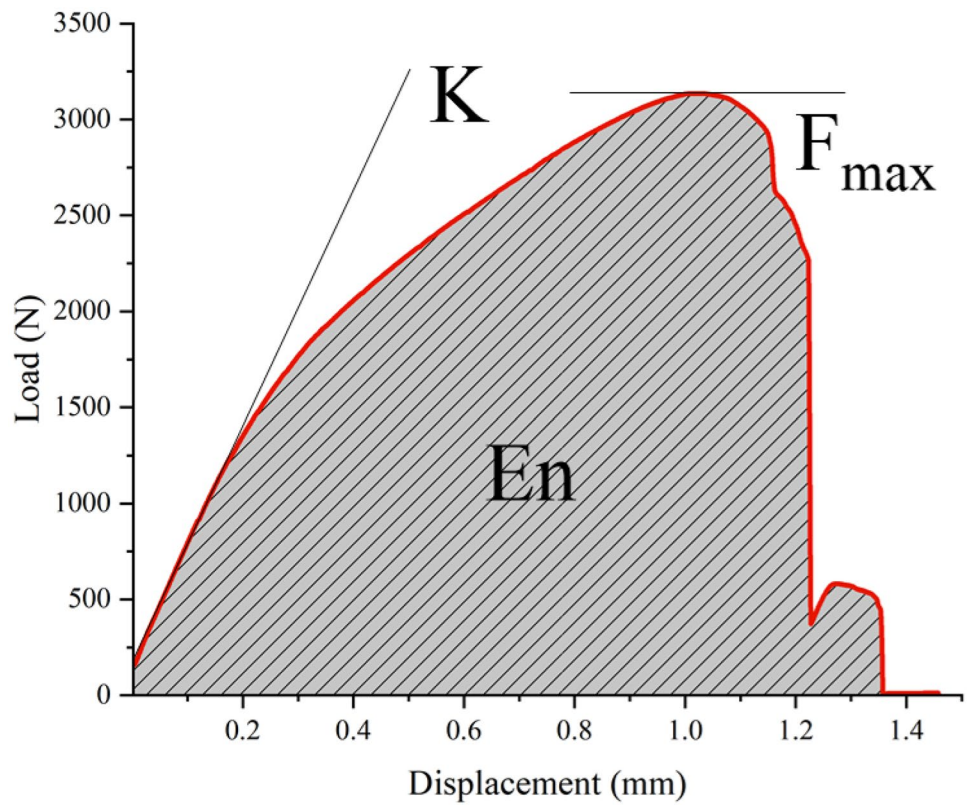


Fig. 5 Specimen configurations in static mechanical tests: **a** cross-tensile test and **b** lap-shear test

Fig. 6 Main mechanical properties of clinched joint reflected in load force–displacement curve



Among these mechanical characteristics, the strength and absorbed energy of clinched structures are of great significance for ensuring the safety of the vehicle passengers.

3 Results and discussion

3.1 Clinch-ability and geometric characteristics

Figure 7 shows the joint sections of various sheet arrangement types and forming forces. As can be noted,

for all sheet arrangements, the mechanical interlocking structure was successfully generated between the upper and lower sheets under the forming forces of 60 kN, 68 kN, and 76 kN. The joints produced from various sheet arrangements were significantly different from each other. There exists an undesired gap between both sheets of A2, B1, C1, and C2 joints, which may be produced due to the poorly coordinated deformation capacity of these dissimilar sheets in the dieless clinching process. In the case of B1 (AL5052-AL6061) sheet arrangement, a wrinkle occurred at the neck of clinched joint, which may lead to local stress

Fig. 7 Joint sections of various sheet arrangement types and forming forces

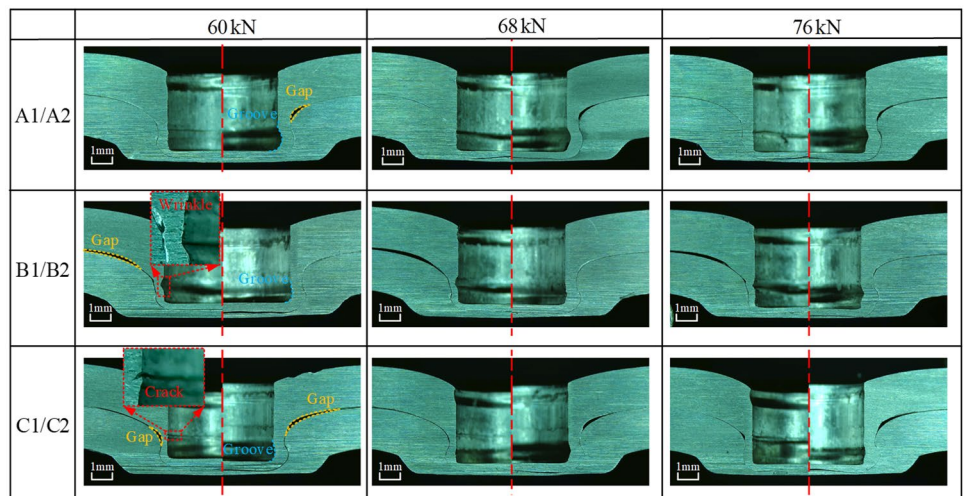
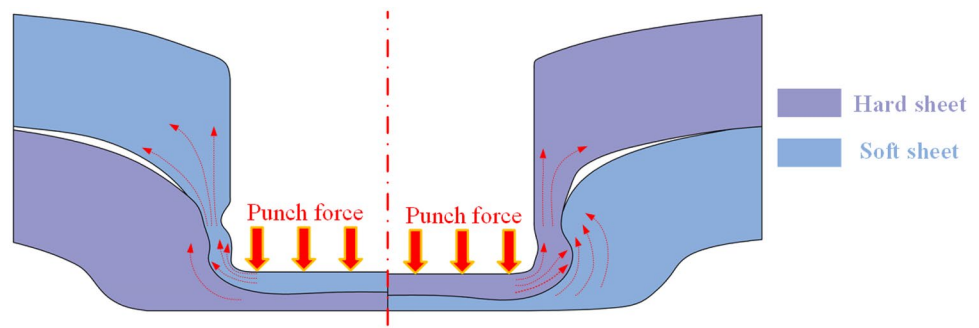


Fig. 8 The material flow behavior of sheet materials



concentration and reduce the joint strength. In the case of C1 (AL5182-AL6061) sheet arrangement, there exists an obvious crack at the joint neck that also may reduce the joint strength. Additionally, for two specific sheet materials, the sequence of sheet placement has a very significant effect on the geometrical shapes of joints. When the upper sheet was characterized with higher resistance to deformation (“harder” intuitively), the clinched joints exhibit greater interlocking structure and neck thickness, while when the upper sheet was characterized with inferior resistance to deformation (“softer” intuitively), some defects, e.g., insufficient interlock value and neck thickness, wrinkle and crack, may occur in the joints produced. Moreover, for all the joints with a hard upper sheet (see the right half of the cross-sections in Fig. 7), a circular groove can be observed near the punch corner. To sum up, for the dieless clinching process for joining dissimilar aluminum sheets, the sheet sequence of the hard upper sheet and soft lower sheet exhibits a better clinch-ability than the sheet sequence of the soft upper sheet and hard lower sheet.

for joining dissimilar sheets. The left half represents the case when the “soft” sheet is at the top and the “hard” sheet is at the bottom while the right half represents the case when the “hard” sheet is at the top and the “soft” sheet is at the bottom. During the dieless clinching process, under the increasing punch force, the upper sheet material was extruded into the lower sheet material. The upper sheet material adjacent to the punch corner was forced to flow upward and radially outwardly, and the lower sheet material adjacent to the punch corner was forced to flow upward and radially inwardly. Both the outwardly radial flow of the upper sheet material and the inwardly radial flow of the lower sheet material led to the formation of an interlocking structure. In the case of “soft” upper sheet and “hard” lower sheet (see the left side of Fig. 8), it is much more difficult to squeeze the upper sheet material into the lower sheet material due to the higher resistance to deformation of the lower sheet. Much upper sheet material near the punch was forced to flow away from the interlock region, and that is why the insufficient interlock structure was induced when the “soft” sheet is at the top. In the case of “hard” upper sheet and “soft” lower sheet (see right side of Fig. 8), the upper sheet material

Figure 8 illustrates the material flow behavior of sheet materials when the dieless clinching process was performed

Fig. 9 Joint neck thicknesses of various sheet arrangement types and forming forces

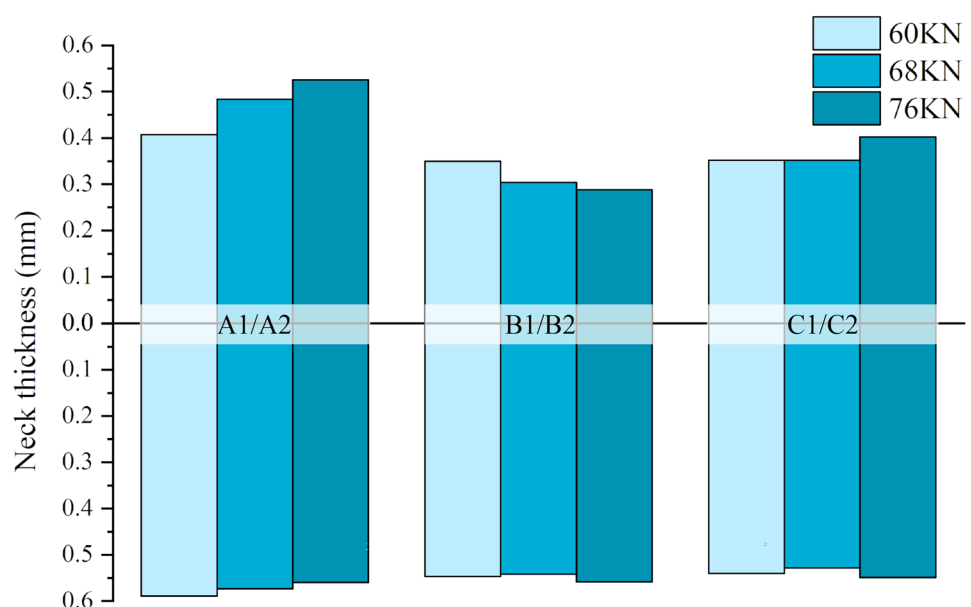
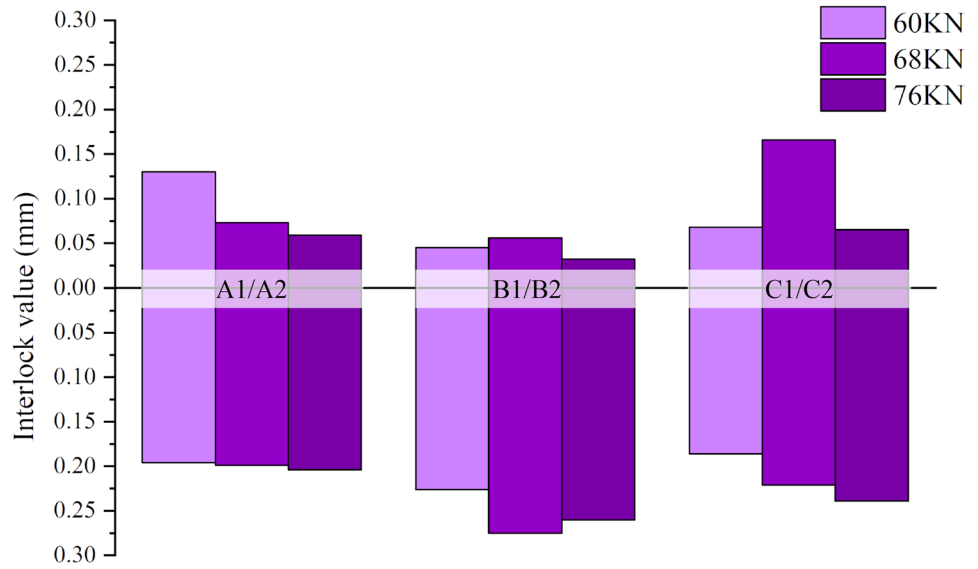


Fig. 10 Joint interlock values of various sheet arrangement types and forming forces



was effortlessly squeezed into the lower sheet material to generate the interlock structure.

A quantitative analysis of the key geometric parameters of the dieless clinched joints in the case of various sheet arrangement types and forming forces was also performed. Figure 9 displays the joint neck thicknesses of various sheet arrangement types and forming forces. As can be observed, both the sheet arrangement types and forming forces have influences on the neck thickness of clinched joints. When the forming force varies from 60 to 76 kN, the joint neck thickness in various sheet arrangements shows different change rules. For example, as the forming force increases from 60 to 76 kN, the neck thickness of the A1 joint is gradually increased while the neck thickness of the A2 joint is continually decreased. In general, the variation of forming

force from 60 to 76 kN has not much effect on the neck thickness of clinched joints.

In Fig. 9, the bars above the horizontal axis represent the neck thickness of joints with a soft upper sheet (A1, B1, and C1 joints) while the bars below the horizontal axis represent the neck thickness of joints with a hard upper sheet (A2, B2, and C2 joints). It can be noted that the joints with a hard upper sheet have larger neck thickness than the joints with a soft upper sheet no matter what the forming force is. When the forming force is 76 kN, the neck thicknesses of A1/A2, B1/B2, and C1/C2 are 0.53 mm/0.56 mm, 0.29 mm/0.56 mm, and 0.40 mm/0.55 mm, respectively. Particularly, when the sheet materials are AL5052 and AL6061, which show the greatest difference in deformation resistance between each other as shown in Fig. 2, the neck

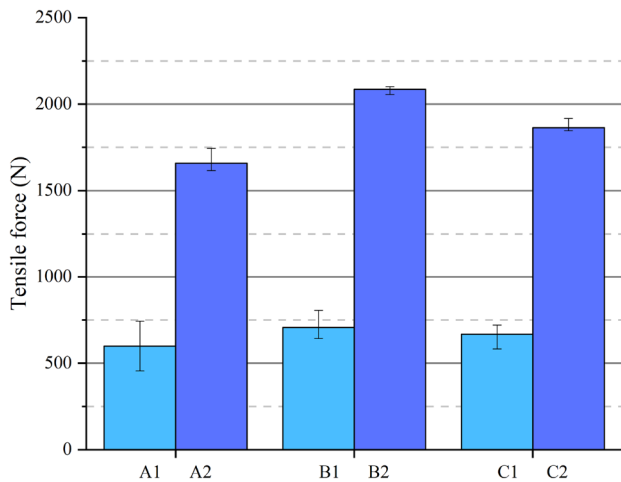


Fig. 11 Tensile strength of the dieless clinched joints in the case of various sheet arrangements

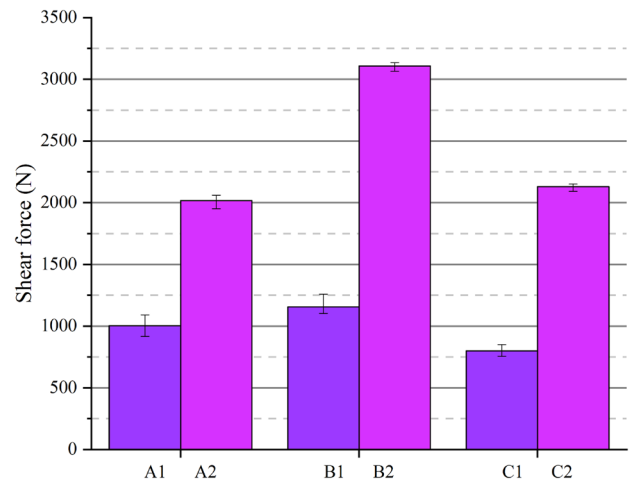


Fig. 12 Shear strength of the dieless clinched joints in the case of various sheet arrangements

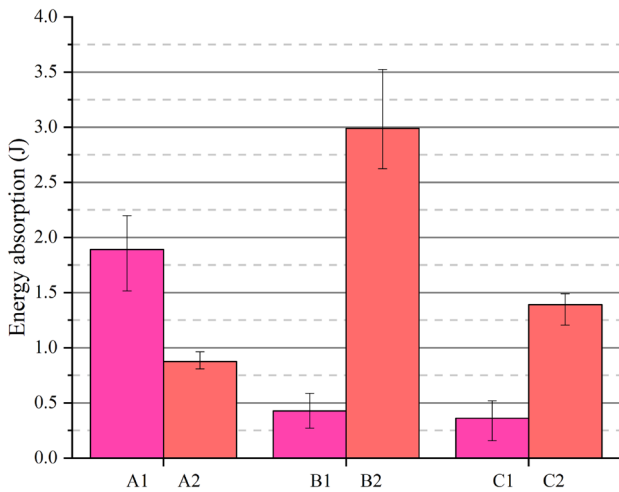


Fig. 13 Energy absorption of the dieless clinched joints in the case of various sheet arrangements

thickness of the AL6061-AL5052 joint (B2 joint) is 93% higher than that of AL5052-AL6061 joint (B1 joint).

Figure 10 shows the joint interlock values of various sheet arrangement types and forming forces. Similar to the joint neck thickness, there exists no consistent change rule regarding the joint interlock values of various sheet arrangements when the forming force varies from 60 to 76 kN. In Fig. 10, the bars above the horizontal axis represent the interlock value of joints with a soft upper sheet (A1, B1, and C1 joints) while the bars below the horizontal axis represent the interlock value of joints with a hard upper sheet (A2, B2, and C2 joints). As can be observed, the joints with a hard upper sheet have a larger interlock value than the joints with a soft upper sheet no matter what the forming force is, which is consistent with the case of the joint neck thickness as shown in Fig. 9. When the forming force is 76 kN, the interlock values of A1/A2, B1/B2, and C1/C2 are 0.06 mm/0.20 mm, 0.03 mm/0.26 mm, and

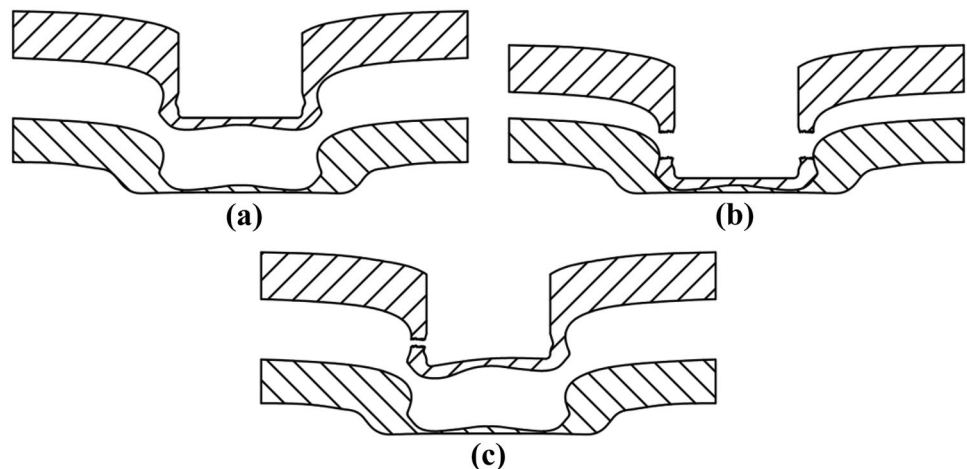
0.07 mm/0.24 mm, respectively. Particularly, when the sheet materials are AL5052 and AL6061, the interlock value of the AL6061-AL5052 joint (B2 joint) is 7.6 times higher than that of the AL5052-AL6061 joint (B1 joint). Compared with the neck thickness, the interlock value of joints is more significantly affected by the sheet combination sequence.

3.2 Strength and energy absorption

To reveal the effect of sheet arrangement types on the mechanical properties of the dieless clinched joints of dissimilar sheets, the static strengths and energy absorptions of clinched joints produced under the uniform 76 kN forming force were analyzed. The tensile strength of the dieless clinched joints in the case of various sheet arrangements is displayed in Fig. 11. As can be noted, the joint tensile strength with a hard upper sheet (A2, B2, and C2 joints) is much higher than that of joints with a soft upper sheet (A1, B1, and C1 joints). And the tensile strength of A2, B2, and C2 joints are 1659 N, 2086 N, and 1864 N respectively, while the tensile strength of A1, B1, and C1 joints are 1148 N, 698 N, and 667 N respectively. Among these joints, the AL6061-AL5052 joint has the maximum tensile strength, which is 199% higher than the tensile strength of the AL5052-AL6061 joint.

The shear strength of the dieless clinched joints in the case of various sheet arrangements is roughly similar to the case of tensile strength as shown in Fig. 12. The shear strength of joints with a hard upper sheet (A2, B2, and C2 joints) is also higher than that of joints with a soft upper sheet (A1, B1, and C1 joints). The shear strength of A2, B2, and C2 joints are 2016 N, 3107 N, and 2130 N respectively, while the shear strength of A1, B1, and C1 joints are 1003 N, 1156 N, and 800 N respectively. Similarly, the AL6061-AL5052 joint also exhibited the maximum tensile strength among these joints.

Fig. 14 Failure modes of the dieless clinched joint: **a** button separation, **b** neck fracture, and **c** button separation company with neck fracture



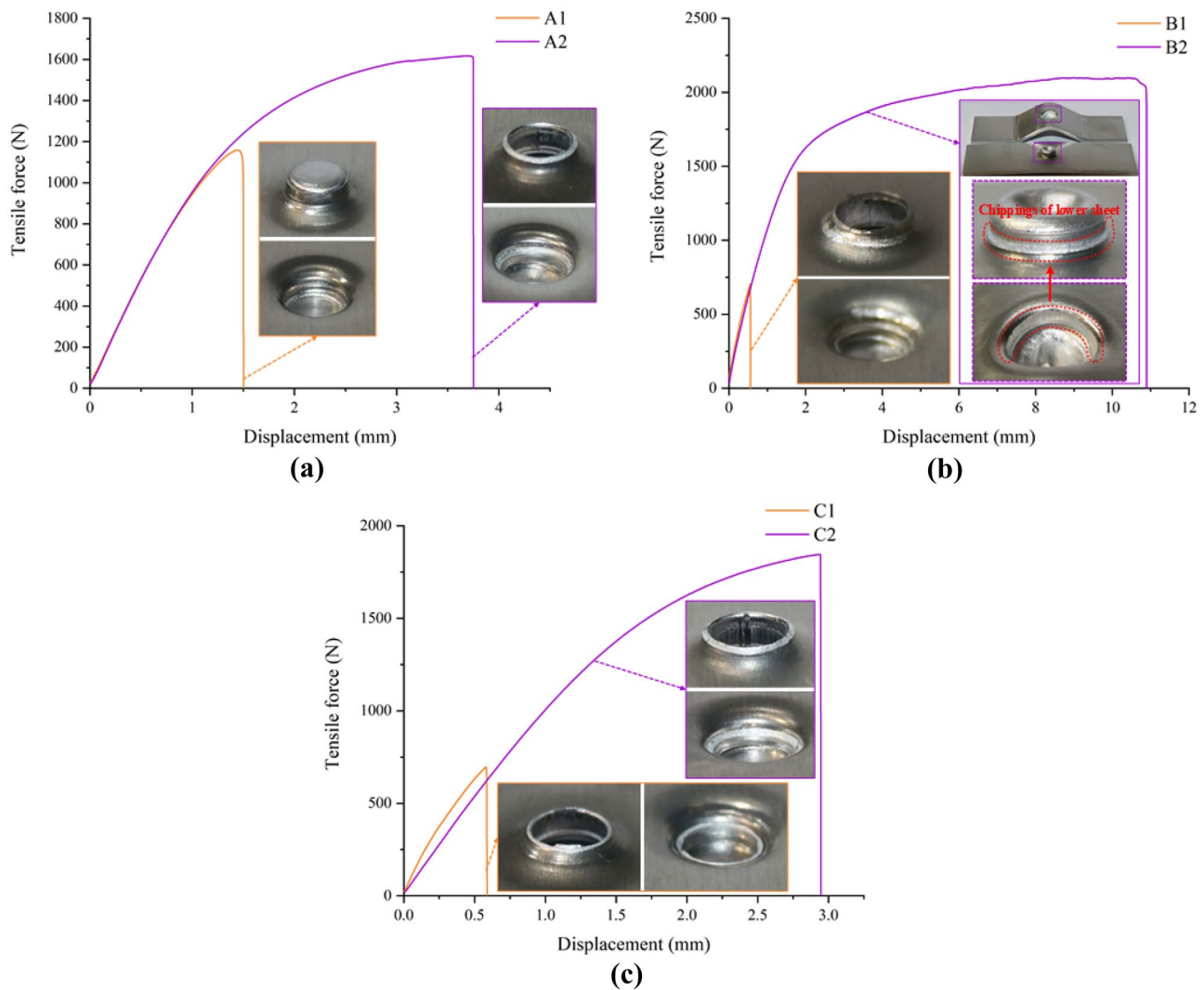


Fig. 15 Load–displacement curves and joint fragments of various joints in cross-tensile test: **a** A1/A2 joints, **b** B1/B2 joints, and **c** C1/C2 joints

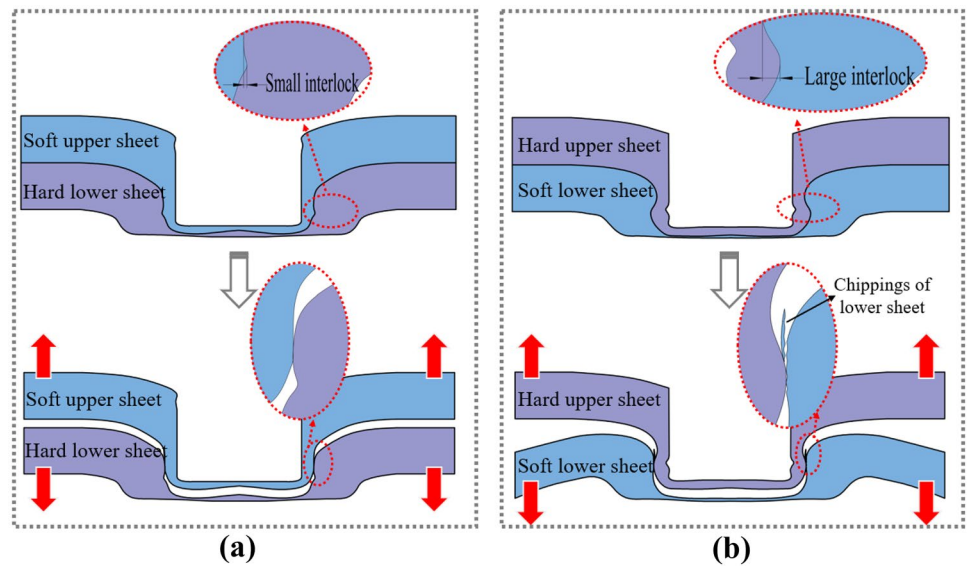
As a critical performance index to improve the crashworthiness of vehicles in a collision and thus ensure passenger safety, the energy absorption of body structure has gained much more and more attention from academics and engineers in the automobile field [27]. For a structure with clinched joint, the absorbed energy is determined by the maximum load and maximum displacement the joint beared and underwent. In the cross-tensile test, the sheets may inevitably bend, which will induce the inaccurate displacement of joint and thus the inaccurate energy absorption. To this end, the absorbed energy of clinched joints in the lap-shear test was merely investigated in this study. Figure 13 displays the energy absorption of the dieless clinched joints in the case of various sheet arrangements. Dissimilar from the case of the static strength shown in Figs. 11 and 12, there exists no consistent law that the energy absorption of the clinched joints with a hard upper sheet is higher than that of joints with a soft upper sheet. When the sheet materials are AL5052 and AL5182, the AL5052-AL5182 joint (A1) exhibits a larger energy absorption value than the AL5182-AL5052

joint (A2) although the AL5182 sheet has a higher resistance to deformation than the AL5052 sheet. When the sheet materials are AL5052/AL6061 (or AL5182/AL6061), the energy absorption of the AL6061-AL5052 joint (or AL6061-AL5182 joint) is much higher than that of the AL5052-AL6061 joint (or AL5182-AL6061 joint), which is consistent with the case of joint static strength shown in Figs. 11 and 12. For all joints of various sheet arrangement types, the AL6061-AL5052 joint has the highest energy absorption (2.99 J), which is approximately 6 times higher than the energy absorption of the AL5052-AL6061 joint (0.43 J).

3.3 Failure modes

According to the previous studies, there exist three typical failure modes concerning the dieless clinched joint after static mechanical tests, i.e., button separation, neck fracture, and button separation company with neck fracture [17]. When the upper sheet is integrally drawn out from the lower sheet,

Fig. 16 Schematic diagram of two types of button separation mode in the cross-tensile test: (a) the case of joint with a soft upper sheet; (b) the case of joint with a hard upper sheet



the joint exhibits a button separation failure mode (Fig. 14a). When the upper sheet is separated from the lower sheet due to the fracture in the joint neck, the joint exhibits a neck fracture mode (Fig. 14b). And when the upper sheet with a partially fractured neck is drawn out from the lower sheet, the joint exhibits the failure mode of button separation company with neck fracture (Fig. 14c). Lei et al. [26] conducted an in-depth and systematic analysis on the failure modes of conventional clinched joints in static mechanical tests, and they reported that the relative strength in the neck and interlock has a decisive impact on the failure modes.

Figures 15 and 17 show the load–displacement curves and joint fragments of various joints in the cross-tensile test and lap-shear test, respectively. From the joint fragments, the failure modes of the dieless clinched joints in the case of various sheet arrangements can be summarized in Table 3. Two types of failure modes, i.e., button separation and neck fracture, occur in these joints. In the cross-tensile test, A1 and B2 joints failed by button separation while A2, B1, C1, and C2 joints failed by neck fracture. In the lap-shear test, A1 joint failed by button separation while other joints failed by neck fracture.

As noted in Fig. 15, all the load–displacement curves of various joints in the cross-tensile test exhibit a similar trend,

i.e., dropping suddenly after reaching their peaks. Moreover, those joints with higher maximum load (tensile strength) also underwent larger displacement in the cross-tensile test. Particularly, the B2 joint (AL6061-AL5052 joint) underwent a displacement up to 11 mm during the cross-tensile test, which was induced by the significant bending deformation occurring in the AL5052 sheet. By observing the B2 joint fragments shown in Fig. 15b, some circular chippings from the lower sheet are located around the neck of the upper sheet.

Although the A1 joint (AL5052-AL5182 joint) and B2 joint (AL6061-AL5052 joint) exhibit the same failure mode in the cross-tensile test, i.e., button separation mode, they went through an entirely different failure process. The A1 joint is considered the joint with a soft upper sheet while the B2 joint is considered the joint with a hard upper sheet. Figure 16 displays the schematic diagram of two types of button separation mode in the cross-tensile test. As can be noted, the joint with a soft upper sheet is characterized by a small interlock while the joint with a hard upper sheet is characterized by a large interlock (see the cross-sections of A1 and B2 joints shown in Fig. 7). During the cross-tensile test, the upper and lower sheet materials at the interlock structure may deform plastically under axial loading. The loads between the upper sheet material and lower sheet material are a pair of loads that is equal and opposite. When the upper sheet

Table 3 Failure modes of the dieless clinched joints in the case of various sheet arrangements

Types of tests	A1	A2	B1	B2	C1	C2	
Cross-tensile test	O	✘	✘	O	✘	✘	O: Button separation mode
Lap-shear test	O	✘	✘	✘	✘	✘	✘: Neck fracture mode

material is softer than the lower sheet material, the small interlock structure may fail easily due to the severe plastic deformation of the upper sheet material, just like the case of A1 joint as shown in Fig. 16a. When the upper sheet material is much harder than the lower sheet material, it is difficult for the upper sheet material at the interlock structure to deform severely or fracture directly. The lower sheet material at the interlock structure will progressively deform until the interlock structure vanishes. Due to the large load the lower sheet bears in this process, the lower sheet will bend, which facilitates the separation of upper and lower sheets. Additionally, some lower sheet material at the interlock structure was directly scraped from the base material by the upper sheet material in the late stage of the joint failure process due to the significant difference in hardness of both sheets (shown in Fig. 16b).

Different from the load–displacement curves in the cross-tensile test, there is no consistent trend for the load–displacement

curves of various joints in the lap-shear test. Additionally, the joints in the lap-shear test also do not comply with the rule that the joints with higher maximum load have greater displacement. When the sheet materials are AL5052/AL5182, the AL5052-AL5182 joint (A1 joint) underwent greater displacement than the AL5182-AL5052 joint (A2 joint), which is why the energy absorption of the former is higher than the latter as shown in Fig. 13.

During the lap-shear test, the joint neck bears an asymmetric shear load, which results in that the clinched joints are easier to fail by neck fracture. Only when the strength in the neck significantly surpasses the strength in the interlock, the clinched joints will fail by button separation. Therefore, all clinched joints except the A1 joint (AL5052-AL5182 joint) exhibit the neck fracture mode in the lap-shear test.

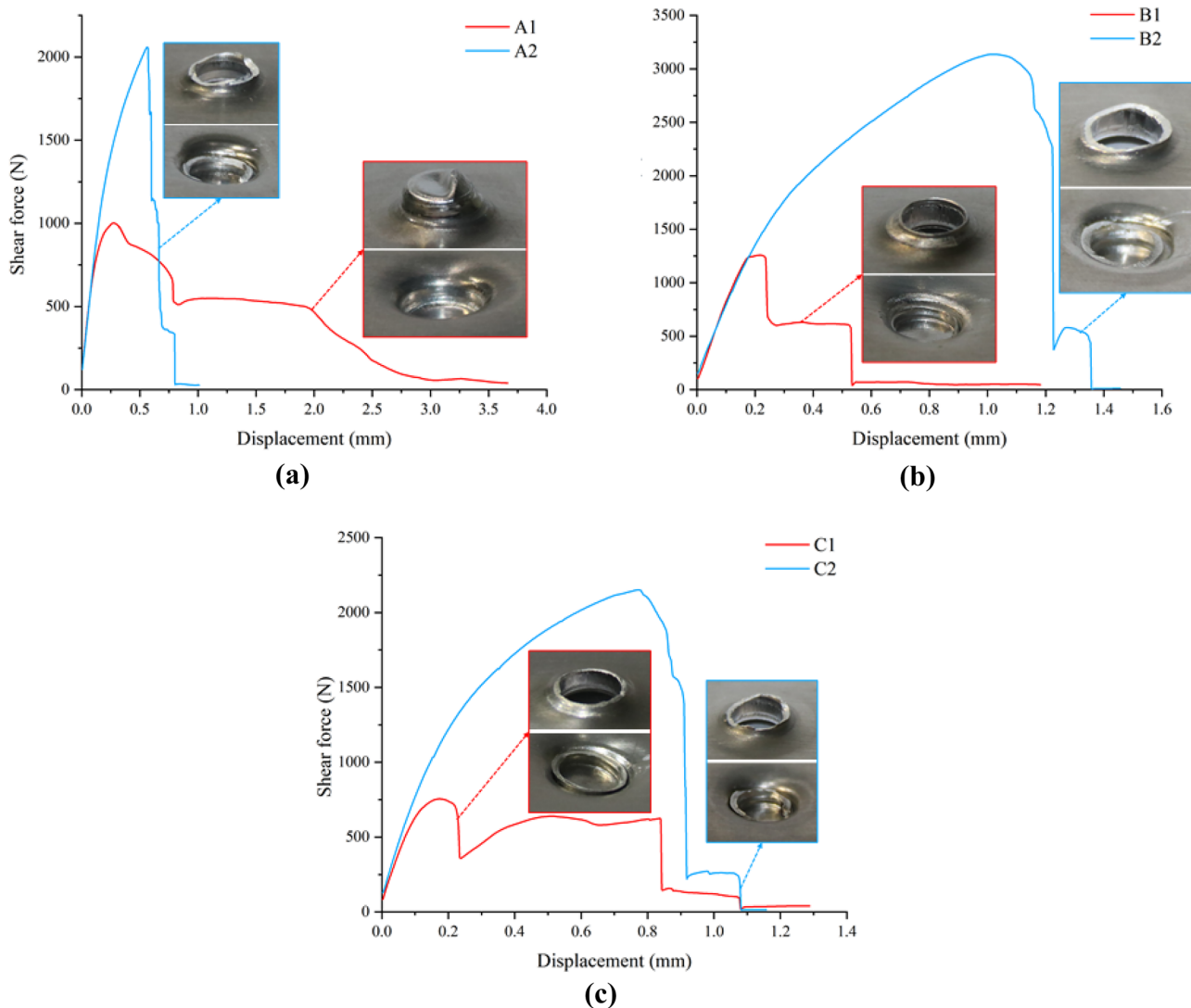


Fig. 17 Load-displacement curves and joint fragments of various joints in lap-shear test: (a) A1/A2 joints; (b) B1/B2 joints; (c) C1/C2 joints

4 Conclusion

In this study, the dieless clinching process for joining dissimilar aluminum alloys was investigated experimentally. Six types of sheet arrangement were prepared to produce the dieless clinched joints. Geometrical analysis upon the cross-sections of various joints was conducted to characterize the clinch-ability of these sheet arrangements. Two types of static mechanical tests, i.e., cross-tensile test and lap-shear test, were conducted to assess the mechanical performance of these joints. The key geometric parameters, static tensile and shear strengths, energy absorptions, and failure modes of these joints were obtained and analyzed. Some conclusions can be drawn from the results as follows:

1. Compared to the forming force, the sheet material arrangements have a more significant impact on the geometry and thus the clinch-ability of the dieless clinched joints. The joints with a hard upper sheet exhibit an adequate neck thickness and interlock value while the joints with a soft upper sheet exhibit some defects, e.g., insufficient interlock value and neck thickness, wrinkle and crack.
2. Sheet material arrangements markedly affect the mechanical performance of the dieless clinched joints. The joints with a hard upper sheet are characterized by higher tensile strength and shear strength. Among the joints of various sheet arrangements, the AL6061-AL5052 joint exhibits the highest static strength and most energy absorption.
3. There are two types of failure modes, i.e., button separation and neck fracture, occurring in these clinched joints in the cross-tensile test and lap-shear test. Although both the AL5052-AL5182 joint and AL6061-AL5052 joint failed by button separation in the cross-tensile test, they went through an entirely different failure process. The failure of the AL5052-AL5182 joint is mainly induced by the plastic deformation of the upper sheet while the failure of the AL6061-AL5052 joint is mainly induced by the plastic deformation of the lower sheet.

Author contribution Denglin Qin carried out the experiments; Denglin Qin and Chao Chen analyzed the data; Chao Chen contributed reagents/materials/analysis tools; Denglin Qin and Chao Chen wrote the paper.

Funding This research work is supported by the National Natural Science Foundation of China (grant no. 51805416), Young Elite Scientists Sponsorship Program by CAST (grant no. 2019QNRC001), Hunan Provincial Natural Science Foundation for Excellent Young Scholars (grant no. 2021JJ20059), Huxiang High-Level Talent Gathering Project of Hunan Province (grant no. 2019RS1002), and the Project of State Key Laboratory of High Performance Complex Manufacturing, Central South University (Grant No. ZZYJKT2022-01).

Data availability The raw/processed data required to reproduce these findings cannot be shared at this time due to technical or time limitations.

Code availability Not applicable.

Declarations

Ethics approval Not applicable.

Consent to participate Not applicable.

Consent for publication Not applicable.

Competing interests The authors declare no competing interests.

References

1. Li J, Wang L, Chen Y, Lu H, Jiang H (2020) Research and application of lightweight index for passenger cars. *Automotive Innovation* 3(3):270–279. <https://doi.org/10.1007/s42154-020-00110-4>
2. Shen Q, Li X, Zhao Y, Gu X, Zou W, Huang X, Mao W (2019) Experimental and performance analyses on elastomer-strengthened polyethylene terephthalate/glass fiber blends. *Automotive Innovation* 2(1):71–78. <https://doi.org/10.1007/s42154-019-00047-3>
3. Li ZC, Deng YL, Yuan MF, Zhang J, Guo XB (2021) Effect of isothermal compression and subsequent heat treatment on grain structures evolution of Al-Mg-Si alloy. *Journal of Central South University* 28(9):2670–2686. <https://doi.org/10.1007/s11771-021-4801-z>
4. Zhang JL, Ye JL, Song B, Li RD, Shi YS (2021) Comparative study on microstructure and electrochemical corrosion resistance of Al7075 alloy prepared by laser additive manufacturing and forging technology. *Journal of Central South University* 28(4):1058–1067. <https://doi.org/10.1007/s11771-021-4679-9>
5. Kalyankar VD, Chudasama GP (2020) Influence of electrode tip diameter on metallurgical and mechanical aspects of spot welded duplex stainless steel. *High Temp Mater Processes (London)* 39(1):317–327. <https://doi.org/10.1515/htmp-2020-0055>
6. Zhang Y, Xu H, Peng R, Lu Y, Zhu L (2021) The state of the art of finite element analysis in mechanical clinching. *Int J Precis Eng Manuf-Green Tech.* <https://doi.org/10.1007/s40684-021-00366-z>
7. Bayraktar M, Cerkez V (2020) Experimental and numerical investigation of clinched joint and implementation of the results to design of a tumble dryer. *J Brazilian Soc Mech Sci Eng* 42(11). <https://doi.org/10.1007/s40430-020-02622-w>
8. Ren XQ, Chen C, Ran XK, Li YX, Zhang XG (2021) Microstructure evolution of AA5052 joint failure process and mechanical performance after reconditioning with tubular rivet. *Trans Nonferr Metal Soc China* 31(11):3380–3393. [https://doi.org/10.1016/S1003-6326\(21\)65736](https://doi.org/10.1016/S1003-6326(21)65736)
9. Neugebauer R, Kraus C, Dietrich S (2008) Advances in mechanical joining of magnesium. *CIRP Ann Manuf Technol* 57(1):283–286. <https://doi.org/10.1016/j.cirp.2008.03.025>
10. Neugebauer R, Todtermuschke M, Mauermann R, Riedel F (2008) Overview on the state of development and the application potential of dieless mechanical joining processes. *Arch Civil Mech Eng* 8(4):51–60. [https://doi.org/10.1016/S1644-9665\(12\)60121-6](https://doi.org/10.1016/S1644-9665(12)60121-6)

11. Neugebauer R, Dietrich S, Kraus C (2007) Dieless clinching and dieless rivet-clinching of magnesium. *Key Eng Mater* 344. <https://doi.org/10.4028/0-87849-437-5.693>
12. Ran X, Chen C, Zhang H, Ouyang Y (2021) Investigation of the clinching process with rectangle punch. *Thin-Walled Structures* 166:108034. <https://doi.org/10.1016/j.tws.2021.108034>
13. Wang C, Kam H, Tan K, Wang X (2021) Study of round and square mechanical clinching joint strength for SPCC steel and aluminium alloy 5052 sheet metal. In *Singapore Adv Mater Sci Eng* Springer Singapore, pp 370–375
14. Gao X, Chen C, Ren X, Li Y (2022) Investigation on failure mechanism of the square clinched joints with different sheet thicknesses. *Eng Fail Anal* 134:106013. <https://doi.org/10.1016/j.engfailanal.2021.106013>
15. Pan Y, Wen T, Zhou Y, You J, Tang H, Chen X (2021) Deformation analysis and processing parameter optimization of roller clinching. *Int J Adv Manuf Technol* 116(5–6):1621–1631. <https://doi.org/10.1007/s00170-021-07215-y>
16. He Y, Yang L, Zong P, Dang J, Ma J (2022) Rotated clinching process for two-layer metallic sheets. *Int J Adv Manuf Technol*. <https://doi.org/10.1007/s00170-021-08474-5>
17. Qin DL, Chen C, Zhang HY, Ren XQ, Wu JL (2021) Experimental investigation of the novel dieless clinching process free of blank holder. *Arch Civ Mech Eng* 22(1). <https://doi.org/10.1007/s43452-021-00347-8>
18. Steinfelder C, Acksteiner J, Guillaume C, Brosius A (2022) Analysis of the interactions between joint and component properties during clinching. *Prod Eng Res Devel*. <https://doi.org/10.1007/s11740-021-01102-x>
19. Lambiase F (2015) Mechanical behaviour of polymer-metal hybrid joints produced by clinching using different tools. *Mater Des* 87:606–618. <https://doi.org/10.1016/j.matdes.2015.08.037>
20. Lambiase F, Paoletti A (2018) Friction-assisted clinching of aluminum and CFRP sheets. *J Manuf Process* 31:812–822. <https://doi.org/10.1016/j.jmapro.2018.01.014>
21. Lambiase F, Ko DC (2017) Two-steps clinching of aluminum and carbon fiber reinforced polymer sheets. *Compos Struct* 164:180–188. <https://doi.org/10.1016/j.compstruct.2016.12.072>
22. Lambiase F, Durante M, Di Ilio A (2016) Fast joining of aluminum sheets with glass fiber reinforced polymer (GFRP) by mechanical clinching. *J Mater Process Technol* 236:241–251. <https://doi.org/10.1016/j.jmatprotec.2016.04.030>
23. Ali B, Benabderrahmane B (2016) Finite element simulation of the hybrid clinch joining. *Int J Adv Manuf Technol* 89(1–4):439–449. <https://doi.org/10.1007/s00170-016-9094-2>
24. Chu MM, He XC, Zhang J, Lei L (2018) Clinching of similar and dissimilar sheet materials of galvanized steel, aluminium alloy and titanium alloy. *Mater Trans* 59(4):694–697. <https://doi.org/10.2320/matertrans.M2017319>
25. Jung JU, Kim SJ, Lee SB, Sim WJ, Kim BG (2021) Mechanical properties of hybrid clinching joints of dissimilar aluminum in electric vehicles. *J Korean Soc Manuf Technol Eng* 30(1):68–73. <https://doi.org/10.7735/ksmte.2021.30.1.68>
26. Lei L, He XC, Yu TX, Xing BY (2019) Failure modes of mechanical clinching in metal sheet materials. *Thin-Walled Structures* 144:106281. <https://doi.org/10.1016/j.tws.2019.106281>
27. Zhang L, Li K, He H, Li LX (2021) Influence of prolonged natural aging followed by artificial aging on tensile properties and compressive behavior of a thin-walled 6005 aluminum alloy tube. *Journal of Central South University* 28(9):2647–2659. <https://link.springer.com/article/10.1007/s11771-021-4799-2>

Publisher's Note Springer Nature remains neutral with regard to jurisdictional claims in published maps and institutional affiliations.

Springer Nature or its licensor holds exclusive rights to this article under a publishing agreement with the author(s) or other rightsholder(s); author self-archiving of the accepted manuscript version of this article is solely governed by the terms of such publishing agreement and applicable law.